Fundamental Toxicological Sciences (Fundam. Toxicol. Sci.)
Vol.9, No.2, 37-46, 2022

The Japanese Society of Toxicology

Fundamental Toxicological Sciences

URL : http://www.fundtoxicolsci.org/index_e.html

Letter

Molecular network analysis of RNA viral infection pathway in diffuse- and intestinal-type gastric cancer

Shihori Tanabe[1], Sabina Quader[2], Ryuichi Ono[3], Horacio Cabral[4], Kazuhiko Aoyagi[5], Akihiko Hirose[1], Hiroshi Yokozaki[6] and Hiroki Sasaki[7]

[1]*Division of Risk Assessment, Center for Biological Safety and Research, National Institute of Health Sciences, 3-25-26 Tonomachi, Kawasaki-ku, Kawasaki 210-9501, Japan*
[2]*Innovation Center of NanoMedicine (iCONM), Kawasaki Institute of Industrial Promotion, 3-25-14 Tonomachi, Kawasaki-ku, Kawasaki 210-0821, Japan*
[3]*Division of Cellular and Molecular Toxicology, Center for Biological Safety and Research, National Institute of Health Sciences, 3-25-26 Tonomachi, Kawasaki-ku, Kawasaki 210-9501, Japan*
[4]*Department of Bioengineering, Graduate School of Engineering, University of Tokyo, 7-3-1 Hongo, Bunkyo-ku, Tokyo 113-0033, Japan*
[5]*Department of Clinical Genomics, National Cancer Center Research Institute, 1-1, Tsukiji 5-chome, Chuo-ku, Tokyo 104-0045, Japan*
[6]*Department of Pathology, Kobe University of Graduate School of Medicine, 7-5-1, Kusunoki-cho, Chuo-ku, Kobe 650-0017, Japan*
[7]*Department of Translational Oncology, National Cancer Center Research Institute, 1-1, Tsukiji 5-chome, Chuo-ku, Tokyo 104-0045, Japan*

(Received March 10, 2022; Accepted March 16, 2022)

ABSTRACT — There are several subtypes of gastric cancer, such as diffuse-type gastric cancer (GC) and intestinal-type GC. Diffuse-type GC is known to be more malignant than intestinal-type GC, showing high metastasis, recurrence and anti-cancer drug resistance. The malignant phenotype of diffuse-type GC includes cancer stem cell (CSC)-like features and epithelial-mesenchymal transition (EMT). By analyzing the molecular network in these tumors, it is possible to reveal the mechanisms of anti-cancer drug resistance, therapeutic targets and drug safety. Upon the analyses of the molecular network in diffuse- and intestinal-type GC, a regulatory network for RNA virus infection was obtained. This study aims to reveal the relationship between cancer and RNA virus infection in detail. RNA virus infection-related molecules and cancer-related molecules were analyzed using network analysis tools, such as Ingenuity Pathway Analysis (IPA), and molecular networks related to RNA virus infection mechanisms. Regulator effect analysis revealed the involvement of RNA virus infection network in diffuse-type GC. c-Jun N-terminal kinase (JNK) and BCL2 like 11 (BCL2L11) in the Coronavirus Pathogenesis Pathway were activated. In conclusion, this research suggested the relationship between the mechanisms of RNA virus infection and diffuse-type GC. This study may be useful for virus infection control and cancer drug discovery by clarifying the relationship between the mechanism of RNA virus infection and cancer.

Key words: Epithelial-mesenchymal transition, Gastric cancer, Molecular network analysis, Pathway network, RNA virus, Therapeutic target

Correspondence: Shihori Tanabe (E-mail: stanabe@nihs.go.jp)

INTRODUCTION

Molecular networks are altered in disease pathogenesis. We have profiled the molecular networks in intestinal- and diffuse-type gastric cancer (GC) to distinguish the subtypes of GC (Tanabe *et al.*, 2020). Upon the molecular network analysis of intestinal- and diffuse-type GC, the regulatory network of RNA virus infection was found to be involved in diffuse-type GC. Further molecular pathway analysis has revealed that several molecules are mapped on the Coronavirus Pathogenesis Pathway, which is activated in diffuse-type GC. To date, the severe acute respiratory syndrome coronavirus 2 (SARS-CoV-2), the new type of coronavirus causing the coronavirus disease 2019 (COVID-19), is a great concern all over the world. SARS-CoV-2 is one of the coronaviruses causing severe symptoms, such as acute respiratory distress syndrome, septic shock, metabolic acidosis, and coagulopathies (Cui *et al.*, 2019; Chen *et al.*, 2020; Tanabe, 2020). Several therapeutic approaches, including RNA-dependent RNA polymerase inhibition and virus neutralization, have been developed to treat the COVID-19 (Florindo *et al.*, 2020; Pizzorno *et al.*, 2020). It has been reported that 16 out of 28 cancer patients with SARS-CoV-2 infection were admitted to hospitals through the emergency departments (Lipe *et al.*, 2020). Moreover, some cancer cases are caused by RNA virus infection, such as human T-cell lymphotropic virus type 1 (HTLV-I) or hepatitis C virus (HCV) (Schiller and Lowy, 2021). Currently, the involvement of cancers in RNA virus infection and coronavirus pathogenesis is not fully revealed. In this study, the relationship between diffuse-type GC and coronavirus pathogenesis pathway is reported.

MATERIALS AND METHODS

Gene expression data of diffuse- and intestinal- type GC

The RNASeq data of diffuse- and intestinal-type GC are publicly available in The cBioPortal for Cancer Genomics database of The Cancer Genome Atlas (TCGA) (Cerami *et al.*, 2012; Gao *et al.*, 2013; Network, 2014) in National Cancer Institute (NCI) Genomic Data Commons (GDC) Data Portal (Grossman *et al.*, 2016). From the publicly available data of stomach adenocarcinoma in TCGA (NCI, USA: https://www.cancer.gov/about-nci/organization/ccg/research/structural-genomics/tcga) (Cerami *et al.*, 2012), intestinal- and diffuse-type GC data, which are noted as chromosomal instability (CIN) (n = 223) and genomically stable (GS) (n = 50), respectively, in TCGA Research Network publication, were compared (Network, 2014).

Molecular network analysis

Data of intestinal- and diffuse-type GC in TCGA cBioPortal Cancer Genomics were uploaded and analyzed through the use of Ingenuity Pathway Analysis (IPA) (QIAGEN Inc., Hilden, Germany) (Krämer *et al.*, 2014).

Gene Ontology (GO) and enrichment analysis

GO was analyzed in the Database for Annotations, Visualization and Integrated Discovery (DAVID) Bioinformatics Resources 6.8 (Laboratory of Human Retrovirology and Immunoinformatics) (Huang da *et al.*, 2009a, 2009b). The total of 2815 probe set IDs were analyzed for enrichment analysis in DAVID as previously described (Tanabe *et al.*, 2020).

Pathway analysis

Canonical pathways were analyzed in diffuse- and intestinal-type GC with IPA as previously described (Tanabe *et al.*, 2021). Coronavirus Pathogenesis Pathway was examined in terms of gene expression in diffuse- and intestinal-type GC. Kyoto Encyclopedia of Genes and Genomes (KEGG) pathway maps were searched by annotation term “hsa05166” that was found to be related to the gene sets (Kanehisa *et al.*, 2022).

Data visualization

The results of gene expression data of RNASeq and network analysis were visualized by Tableau software (https://www.tableau.com).

Statistical analysis

The RNASeq data were analyzed by Student’s t-test. Z-score in intestinal- and diffuse-type GC samples were compared, and the difference was considered to be significant in p value $< 10^{-5}$. For DAVID GO enrichment analysis, data was analyzed in the default setting (Huang da *et al.*, 2009a, 2009b). GO enrichment was considered significant in modified Fischer Exact p value $< 10^{-6}$. Bonferroni statistics showed p value < 0.005.

RESULTS AND DISCUSSION

Regulator effect analysis revealed the involvement of RNA virus infection network in diffuse-type GC

Regulator effect analysis of 2815 genes altered in diffuse- and intestinal-type GC revealed the involvement of RNA virus infection network in diffuse-type GC (Fig. 1). In this network, protein kinase C beta (PRKCB) in protein kinase C (PKC) group was identified as a link molecule to a canonical pathway of the virus entry *via* endocytotic pathways. PRKCB is involved in ligand-dependent nucle-

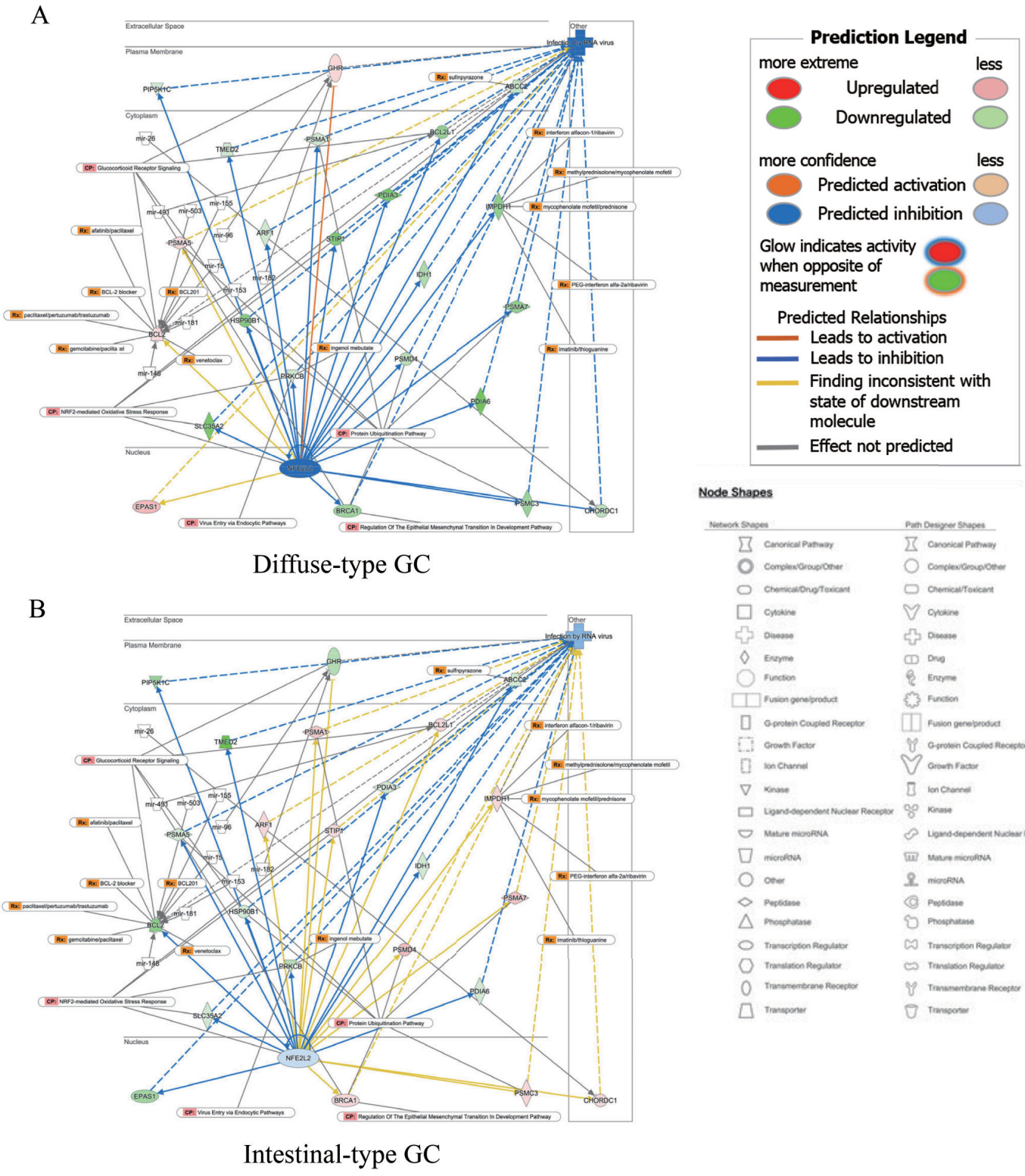

Fig. 1. Regulator effect analysis revealed the involvement of RNA virus infection network in diffuse-type GC. (A) Infection by RNA virus network identified in regulator effect analysis in diffuse-type GC. (B) Infection by RNA virus network identified in regulator effect analysis in intestinal-type GC. The genes whose expression was altered in diffuse- and intestinal-type GC are shown in pink (upregulated) or green (downregulated). Predicted activation and inhibition are shown in orange and blue, respectively.

ar receptor transcription as a co-activator. PKC phosphorylates a variety of proteins involved in diverse cellular signaling pathways. PRKCB has been found to be related to a signaling network of SARS-CoV-2 (More *et al.*, 2021). Nuclear factor, erythroid 2 like 2 (NFE2L2) was identified as a master regulator of 23 molecules, ABCC2, ARF1, BCL2, BCL2L1, BRCA1, CHORDC1, EPAS1, GHR, HSP90B1, IDH1, IMPDH1, PDIA3, PDIA6, PIP5K1C, PRKCB, PSMA1, PSMA5, PSMA7, PSMC3, PSMD4, SLC35A2, STIP1, TMED2, which have relationship with the infection of RNA virus in the molecular network. NFE2L2, a transcription factor and a member of a small family of basic leucin zipper (bZIP) proteins, is involved in the detoxification of reactive oxygen species (ROS) (Schäfer *et al.*, 2010).

Coronavirus pathogenesis pathway was activated in diffuse-type GC

Since our previous study has revealed that the coronavirus pathogenesis pathway was altered in diffuse- and intestinal-type GC (Tanabe *et al.*, 2021), the activation states of coronavirus pathogenesis pathway in diffuse- and intestinal-type GC were analyzed. Coronavirus pathogenesis pathway was activated in diffuse-type GC compared to intestinal-type GC (Fig. 2). BCL2 apoptosis regulator (BCL2) and c-Jun N-terminal kinase (JNK) were up-regulated in diffuse-type GC compared to intestinal-type GC. A JNK node includes MAP2K4, MAPK10, MAPK12, MAPK8 and MAPK9 in IPA analysis. MAPK8 corresponds to JNK1, whereas MAPK10 corresponds to JNK or JNK3. SMAD family member 3 (SMAD3) and serpin family E member 1 (SERPINE1) were predicted as activated in diffuse-type GC compared to intestinal-type GC. Signal transducer and activator of transcription 1 (STAT1), ISGF3, karyopherin subunit β (KPNB), and interferon regulatory factor 3 (IRF3) were down-regulated in diffuse-type GC compared to intestinal-type GC. IRF7 was predicted as inactivated in diffuse-type GC compared to intestinal-type GC. We have found that the possible therapeutic targets include JNK family and BCL2 pathways. In the setting of renin-angiotensin system in COVID-19, angiotensin II, which is involved in JNK activation, plays an important role to angiotensin-converting enzyme 2 (ACE2) internalization (Edmonston *et al.*, 2020). JNK is found to be activated in coronavirus infection, which leads to apoptosis and induction of pro-inflammatory cytokines, such as interleukin-6 (IL-6) (Banerjee *et al.*, 2002; Fung *et al.*, 2016). BCL2, a regulator of apoptosis, plays an important role in cancer development (Alam *et al.*, 2021). A computational prediction has revealed that BCL2 is targeted by SARS-CoV-2 encoded miRNAs (Aydemir *et al.*, 2021). The computation analysis also predicted that SARS-CoV-2 encoded miRNAs target the genes identified as related to coronavirus pathogenesis pathway in diffuse- and intestinal-type GC: JAK1, NFKB1, SMAD3, SMAD4 and HDAC2 (Aydemir *et al.*, 2021).

Molecules related to coronavirus pathogenesis pathway in diffuse- and intestinal-type GC

Table 1 shows molecules related to the coronavirus pathogenesis pathway in the canonical pathway of IPA comparison analysis. Gene expression of molecules related to coronavirus pathogenesis pathway in diffuse- and intestinal-type GC are also shown in Table 1. A total of 32 molecules are altered in diffuse- and intestinal-type GC, as shown with the biomarker application. The molecules having an alteration in the gene expression were kinase, transcription regulator, transmembrane receptor, transporter, and others (Table 1). Biomarker application included efficacy, response to therapy for ABL proto-oncogene 1, non-receptor tyrosine kinase (ABL1), diagnosis for cyclin dependent kinase 4 (CDK4), efficacy for Janus kinase 1 (JAK1), diagnosis, efficacy, prognosis, response to therapy, unspecified application for cyclin D1 (CCND1), disease progression and prognosis for E2F transcription factor 1 (E2F1), prognosis for SMAD4, diagnosis, efficacy, prognosis, and response to therapy for STAT1, diagnosis, efficacy, and prognosis for BCL2. Belinostat, chidamide, pyroxamide, and tributyrin are drugs targeting HDAC2 and HDAC10.

GO enrichment analysis of molecules altered in diffuse- and intestinal-type GC

GO enrichment analysis identified 7 terms of GO molecular function regulated in diffuse- and intestinal-type GC (Table 2, Fig. 3). The total of 2815 probe set IDs were analyzed for enrichment analysis in DAVID, which resulted in 2412 genes analyzed in GO molecular function. Category of GOTERM_MF_DIRECT is listed in Table 2. Molecular functions of protein binding, poly(A) RNA binding, ATP binding, RNA binding, DNA binding, chromatin binding, and threonine-type endopeptidase activity were significantly enriched in the altered gene sets of diffuse- and intestinal-type GC. GO enrichment was considered significant in modified Fischer Exact p value $< 10^{-6}$. The color in Fig. 3 indicates fold enrichment value, which ranges from 1.171 (in blue) to 5.312 (in red). Molecules enriched in threonine-type endopeptidase activity included proteasome 20S subunit and taspase 1 (TASP1).

A

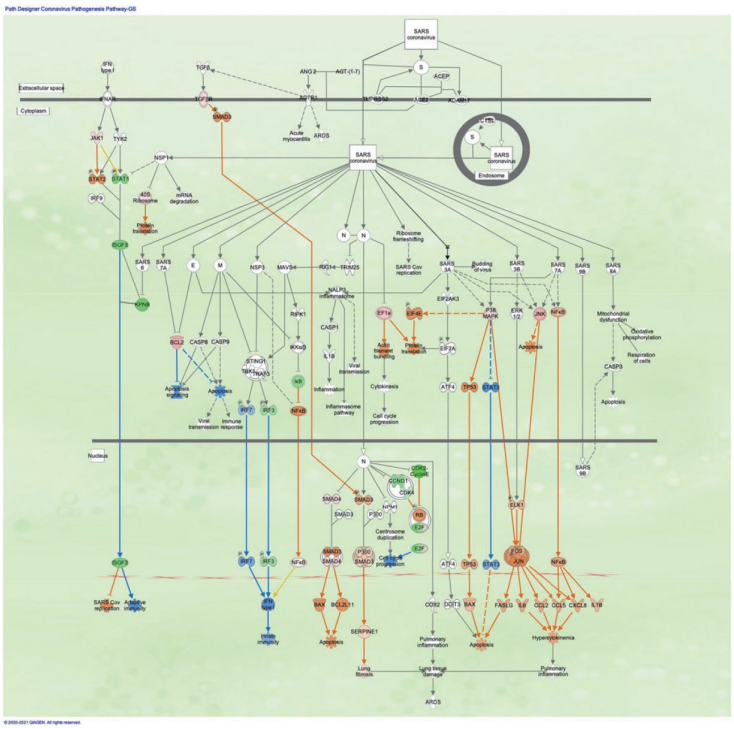

Diffuse-type GC

B

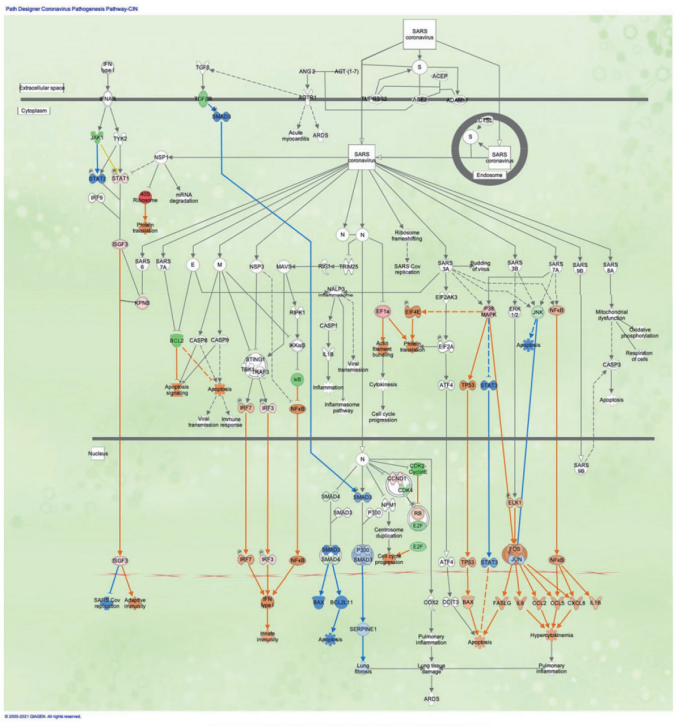

Intestinal-type GC

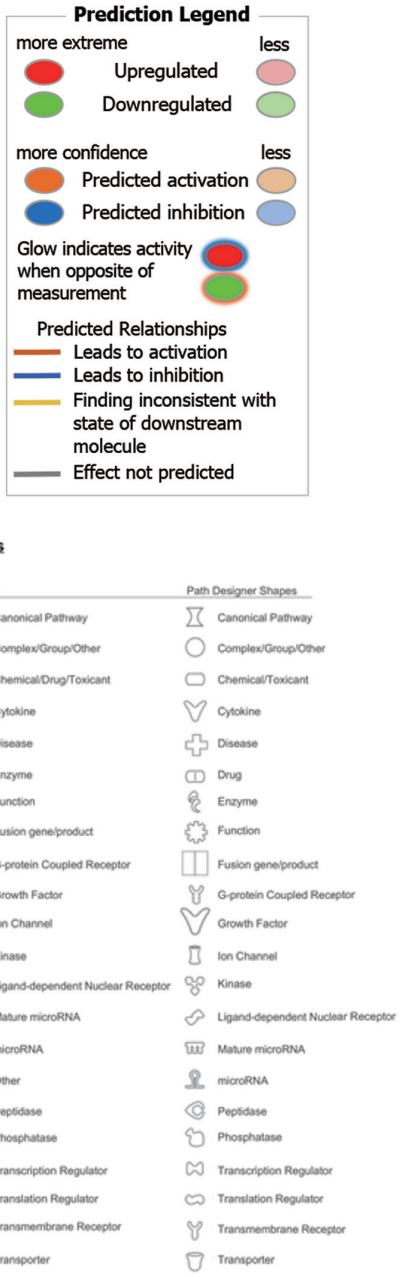

Fig. 2. Coronavirus pathogenesis pathway in diffuse- and intestinal-type GC. (A) Coronavirus pathogenesis pathway (IPA) in diffuse-type GC. (B) Coronavirus pathogenesis pathway (IPA) in intestinal-type GC. The genes with altered expression in diffuse- and intestinal-type GC are shown in pink (upregulated) or green (downregulated). Predicted activation and inhibition are shown in orange and blue, respectively.

Table 1. Molecules related to coronavirus pathogenesis pathway with altered expression in diffuse- and intestinal-type GC.

Symbol	Entrez Gene Name	Expr Other (diffuse-type GC)	Expr Other (intestinal-type GC)	Location	Biomarker Application(s)	Type(s)
ABL1	ABL proto-oncogene 1, non-receptor tyrosine kinase	0.485	−0.332	Nucleus	efficacy, response to therapy, unspecified application	kinase
CDK2	cyclin dependent kinase 2	−1.591	−1.002	Nucleus		
CDK4	cyclin dependent kinase 4	−0.372	−0.534	Nucleus	diagnosis	
JAK1	Janus kinase 1	0.249	−1.001	Cytoplasm	efficacy	
MAPK10	mitogen-activated protein kinase 10	0.931	−0.302	Cytoplasm		
MAPK13	mitogen-activated protein kinase 13	0.172	0.686	Cytoplasm		
TGFBR2	transforming growth factor beta receptor 2	0.181	−0.747	Plasma Membrane		
CCND1	cyclin D1	−0.72	0	Nucleus	diagnosis, efficacy, prognosis, response to therapy, unspecified application	transcription regulator
CCNE1	cyclin E1	−0.58	26.977	Nucleus		
E2F1	E2F transcription factor 1	−0.943	3.081	Nucleus	disease progression, prognosis	
E2F3	E2F transcription factor 3	−0.182	1.097	Nucleus	unspecified application	
E2F4	E2F transcription factor 4	−0.634	−0.603	Nucleus		
E2F5	E2F transcription factor 5	0.22	1.523	Nucleus		
E2F6	E2F transcription factor 6	−0.675	5.398	Nucleus		
E2F7	E2F transcription factor 7	−1.067	0.151	Nucleus		
E2F8	E2F transcription factor 8	−0.936	0.585	Nucleus		
HDAC10	histone deacetylase 10	−1.064	−0.193	Nucleus		
HDAC2	histone deacetylase 2	0.212	2.425	Nucleus		
IRF3	interferon regulatory factor 3	−0.581	0.194	Nucleus		
NFKBIB	NFKB inhibitor beta	−0.672	−0.836	Nucleus		
PA2G4	proliferation-associated 2G4	−0.105	−0.475	Nucleus		
PTGES2	prostaglandin E synthase 2	1.324	4.253	Cytoplasm		
SMAD4	SMAD family member 4	0.168	−0.043	Nucleus	prognosis, unspecified application	
STAT1	signal transducer and activator of transcription 1	−0.875	0.299	Nucleus	diagnosis, efficacy, prognosis, response to therapy	
TFDP1	transcription factor Dp-1	−0.793	−0.604	Nucleus		
EEF1A1	eukaryotic translation elongation factor 1 alpha 1	0.693	0.893	Cytoplasm		
SIGMAR1	sigma non-opioid intracellular receptor 1	0.209	0.02	Plasma Membrane		transmembrane receptor
ATP6AP1	ATPase H^+ transporting accessory protein 1	−0.14	−0.902	Cytoplasm		transporter
BCL2	BCL2 apoptosis regulator	0.998	−0.974	Cytoplasm	diagnosis, efficacy, prognosis, unspecified application	
CCNE2	cyclin E2	−0.278	−0.222	Nucleus		other
KPNB1	karyopherin subunit beta 1	−1.091	0.021	Nucleus		
RPS21	ribosomal protein S21	0.301	2.395	Cytoplasm		

Molecules related to coronavirus pathogenesis pathway in IPA comparison analysis and their expression in diffuse- and intestinal-type GC are shown.

Table 2. GO molecular function of genes regulated in intestinal-and diffuse-type GC.

Term	Count	%	*p* value	Fold Enrichment
GO:0005515~protein binding	1558	56.41	1.60E-41	1.24
GO:0044822~poly(A) RNA binding	297	10.75	3.45E-28	1.84
GO:0005524~ATP binding	309	11.19	1.86E-12	1.45
GO:0003723~RNA binding	133	4.82	3.32E-10	1.70
GO:0003677~DNA binding	313	11.33	1.23E-07	1.31
GO:0003682~chromatin binding	94	3.40	2.79E-07	1.68
GO:0004298~threonine-type endopeptidase activity	14	0.51	6.58E-07	4.67

The total of 2815 probe set IDs were analyzed for enrichment analysis in DAVID, which resulted in 2412 genes analyzed in GO Molecular Function. Category of GOTERM_MF_DIRECT is listed.

Table 3. KEGG pathway related to RNA viral infection in DAVID.

Category	KEGG_PATHWAY
Term	hsa05166: HTLV-I infection
Count	50
%	1.8102824
p value	0.01590334
Genes	CRTC2, WNT2B, BUB1B, PIK3CB, CDC20, XPO1, PTTG1, CCND1, CHEK2, AKT3, PRKACB, JAK1, PDGFRA, MSX2, ANAPC7, TGFBR2, KAT2B, KAT2A, MRAS, ADCY9, CANX, TLN1, VAC14, PCNA, ADCY4, PIK3R1, ANAPC11, WNT11, POLD2, DVL1, E2F1, E2F3, FZD1, STAT5A, RANBP1, MAP3K3, STAT5B, SMAD4, FZD4, CDKN2A, NFATC4, APC, CDK4, POLE2, POLE3, CALR, LTBR, RAN, BCL2L1, MAD2L1
List Total	986
Pop Hits	254
Pop Total	6879
Fold Enrichment	1.37336091
Bonferroni	0.98894368
Benjamini	0.17187835
FDR	0.15964502

GO enrichment analysis with DAVID showed that human T-cell leukemia virus 1 (HTLV-I) infection (KEGG pathway) is involved in molecules altered in diffuse- and intestinal-type GC.

GO and pathway analysis related to RNA virus in molecules altered in diffuse- and intestinal-type GC

GO and pathway analysis related to RNA virus revealed that HTLV-I infection (KEGG pathway) is involved in molecules altered in diffuse- and intestinal-type GC (Fig. 4). Functional annotation in DAVID found that HTLV-I infection in KEGG pathway had a fold enrichment value of 1.373 (Table 3). The genes identified by DAVID in the KEGG HTLV-I infection pathway included CRTC2, WNT2B, BUB1B, PIK3CB, CDC20, XPO1, PTTG1, CCND1, CHEK2, AKT3, PRKACB, JAK1, PDGFRA, MSX2, ANAPC7, TGFBR2, KAT2B, KAT2A, MRAS, ADCY9, CANX, TLN1, VAC14, PCNA, ADCY4, PIK3R1, ANAPC11, WNT11, POLD2, DVL1, E2F1, E2F3, FZD1, STAT5A, RANBP1, MAP3K3, STAT5B, SMAD4, FZD4, CDKN2A, NFATC4, APC, CDK4, POLE2, POLE3, CALR, LTBR, RAN, BCL2L1 and MAD2L1 (Table 3, Fig. 4). MAPK8/JNK1 is located in the TNF signaling pathway of the HTLV-I infection pathway. JAK1 is downstream of IL2R leading to T cell activation in the HTLV-I infection pathway. HTLV-I infection shares pathways with SARS-CoV-2 infection, which is also involved in DNA virus Epstein-Barr virus and influenza A, etc. (Barh *et al.*, 2020). Multi-omics data analysis of SARS-CoV-2 infection revealed that HTLV-I infection pathway is enriched in at least three omics data sets in five omics data sets of interactome, transcriptome, proteome, and bibliome (Barh *et al.*, 2020). Viral targeting of PDZ (postsynaptic density protein 95 (PSD95), discs large (Dlg), zonula occludens (ZO)-1) domain-containing proteins induce T-cell transformation and proliferation, and persistent HTLV-1 infection (Gutierrez-Gonzalez and Santos-Mendoza, 2019). SARS-CoV encodes viroporins with PDZ binding-motif, which is involved in virus replication and pathogenesis (Castano-Rodriguez *et al.*, 2018). ROS production by NADPH oxidase complex depends on PDZ-

Fig. 3. GO enrichment analysis with DAVID identified 7 terms of GO molecular function regulation in diffuse- and intestinal-type GC. The total of 2815 probe set IDs were analyzed for enrichment analysis in DAVID, which resulted in 2412 genes analyzed in GO molecular function. p value $< 10^{-6}$ was considered as significant. The color indicates fold enrichment value, which ranges from 1.171 (in blue) to 5.312 (in red).

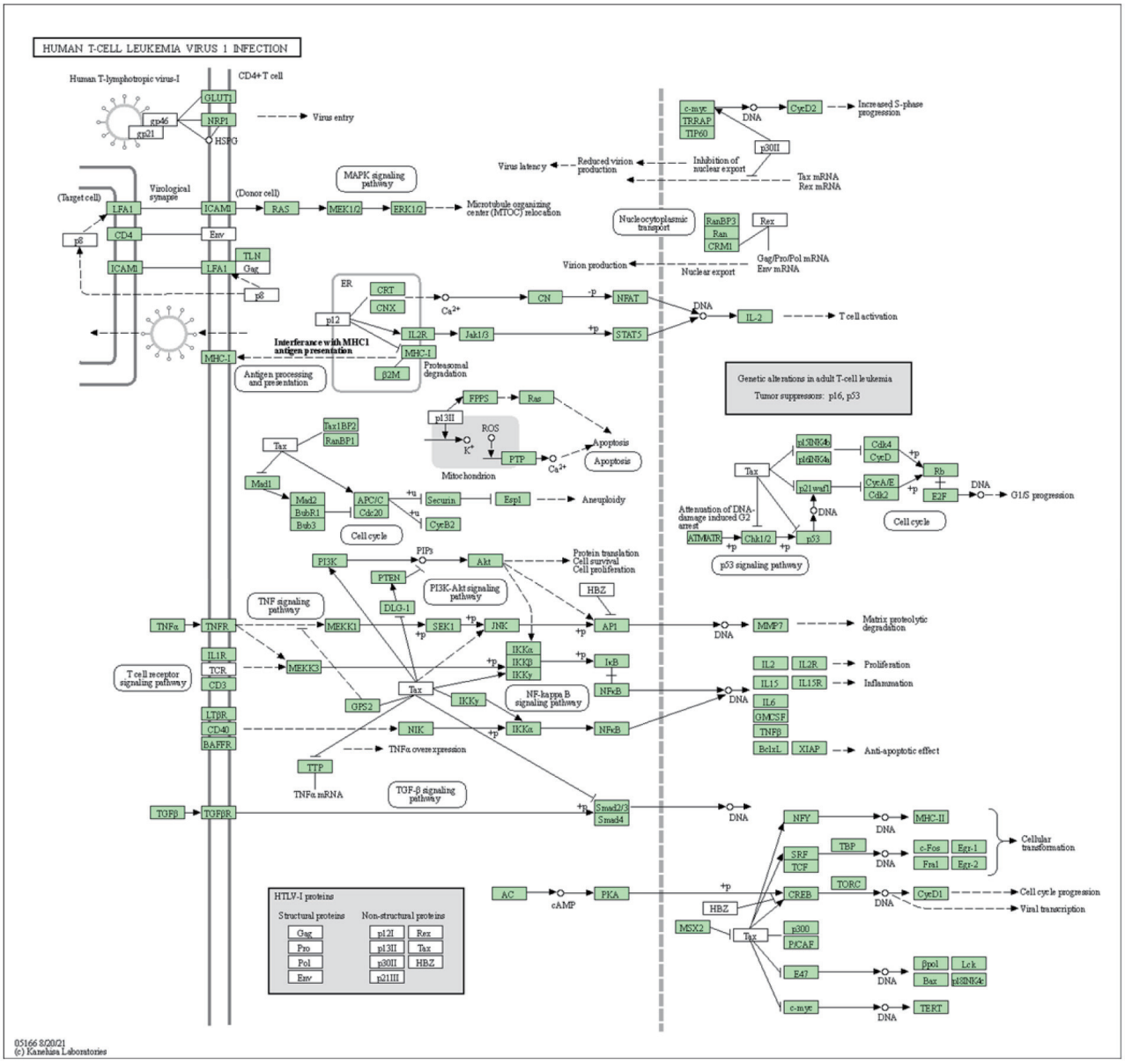

Fig. 4. HTLV-I infection (KEGG pathway). Kyoto Encyclopedia of Genes and Genomes (KEGG) pathway maps were searched by annotation term "hsa05166" that was found to be related to the genes altered in diffuse- and intestinal-type GC. KEGG pathway "Human T-cell leukemia virus 1 infection" (hsa05166) is shown.

domain in bacterial infection (Zheng *et al.*, 2016). Since PDZ domain-containing proteins play a role in cellular polarity, EMT may be induced by PDZ domain-containing proteins (Qi *et al.*, 2020). In conclusion, this study demonstrates the result of molecular network analysis of diffuse- and intestinal-type GC in coronavirus pathogenesis pathway and RNA virus infection. The results propose the relationship between diffuse-type GC and RNA viral infection, for which further investigation is needed. The involvement of JNK and BCL2 pathways in RNA virus and cancer would be the future direction of the research.

ACKNOWLEDGMENTS

This work was supported by Japan Agency for Medical Research and Development (AMED), Grant Numbers

JP21mk0101216 (S.T.), JP20ak0101093 (S.T., R.O. and A.H.) and JP20mk0101163 (RO), and Strategic International Collaborative Research Program, Grant Number JP20jm0210059 (S.T. and S.Q.), Ministry of Health, Labour, and Welfare (MHLW), Grant Number H30-KAGAKU-IPPAN-002 (S.T. and R.O.), and JSPS KAKENHI Grant Number 21K12133 (S.T. and R.O.).

Conflict of interest---- The authors declare that there is no conflict of interest.

REFERENCES

Alam, M., Ali, S., Mohammad, T., Hasan, G.M., Yadav, D.K. and Hassan, M.I. (2021): B Cell Lymphoma 2: A Potential Therapeutic Target for Cancer Therapy. Int. J. Mol. Sci., **22**, 10442.

Aydemir, M.N., Aydemir, H.B., Korkmaz, E.M., Budak, M., Cekin, N. and Pinarbasi, E. (2021): Computationally predicted SARS-COV-2 encoded microRNAs target NFKB, JAK/STAT and TGFB signaling pathways. Gene Rep., **22**, 101012.

Banerjee, S., Narayanan, K., Mizutani, T. and Makino, S. (2002): Murine coronavirus replication-induced p38 mitogen-activated protein kinase activation promotes interleukin-6 production and virus replication in cultured cells. J. Virol., **76**, 5937-5948.

Barh, D., Tiwari, S., Weener, M.E., Azevedo, V., Goes-Neto, A., Gromiha, M.M. and Ghosh, P. (2020): Multi-omics-based identification of SARS-CoV-2 infection biology and candidate drugs against COVID-19. Comput. Biol. Med., **126**, 104051.

Castano-Rodriguez, C., Honrubia, J.M., Gutierrez-Alvarez, J., DeDiego, M.L., Nieto-Torres, J.L., Jimenez-Guardeno, J.M., Regla-Nava, J.A., Fernandez-Delgado, R., Verdia-Baguena, C., Queralt-Martin, M., Kochan, G., Perlman, S., Aguilella, V.M., Sola, I. and Enjuanes, L. (2018): Role of Severe Acute Respiratory Syndrome Coronavirus Viroporins E, 3a, and 8a in Replication and Pathogenesis. MBio, **9**, e02325-17.

Cerami, E., Gao, J., Dogrusoz, U., Gross, B.E., Sumer, S.O., Aksoy, B.A., Jacobsen, A., Byrne, C.J., Heuer, M.L., Larsson, E., Antipin, Y., Reva, B., Goldberg, A.P., Sander, C. and Schultz, N. (2012): The cBio Cancer Genomics Portal: An Open Platform for Exploring Multidimensional Cancer Genomics Data. Cancer Discov., **2**, 401-404.

Chen, B., Tian, E.-K., He, B., Tian, L., Han, R., Wang, S., Xiang, Q., Zhang, S., El Arnaout, T. and Cheng, W. (2020): Overview of lethal human coronaviruses. Signal Transduct. Target. Ther., **5**, 89.

Cui, J., Li, F. and Shi, Z.-L. (2019): Origin and evolution of pathogenic coronaviruses. Nat. Rev. Microbiol., **17**, 181-192.

Edmonston, D.L., South, A.M., Sparks, M.A. and Cohen, J.B. (2020): Coronavirus Disease 2019 and Hypertension: The Role of Angiotensin-Converting Enzyme 2 and the Renin-Angiotensin System. Adv. Chronic Kidney Dis., **27**, 404-411.

Florindo, H.F., Kleiner, R., Vaskovich-Koubi, D., Acúrcio, R.C., Carreira, B., Yeini, E., Tiram, G., Liubomirski, Y. and Satchi-Fainaro, R. (2020): Immune-mediated approaches against COVID-19. Nat. Nanotechnol., **15**, 630-645.

Fung, T.S., Liao, Y. and Liu, D.X. (2016): Regulation of Stress Responses and Translational Control by Coronavirus. Viruses, **8**, 184.

Gao, J., Aksoy, B.A., Dogrusoz, U., Dresdner, G., Gross, B., Sumer, S.O., Sun, Y., Jacobsen, A., Sinha, R., Larsson, E., Cerami, E., Sander, C. and Schultz, N. (2013): Integrative analysis of complex cancer genomics and clinical profiles using the cBioPortal. Sci. Signal., **6**, pl1.

Grossman, R.L., Heath, A.P., Ferretti, V., Varmus, H.E., Lowy, D.R., Kibbe, W.A. and Staudt, L.M. (2016): Toward a Shared Vision for Cancer Genomic Data. N. Engl. J. Med., **375**, 1109-1112.

Gutierrez-Gonzalez, L.H. and Santos-Mendoza, T. (2019): Viral targeting of PDZ polarity proteins in the immune system as a potential evasion mechanism. FASEB J., **33**, 10607-10617.

Huang da, W., Sherman, B.T. and Lempicki, R.A. (2009a): Bioinformatics enrichment tools: paths toward the comprehensive functional analysis of large gene lists. Nucleic Acids Res., **37**, 1-13.

Huang da, W., Sherman, B.T. and Lempicki, R.A. (2009b): Systematic and integrative analysis of large gene lists using DAVID bioinformatics resources. Nat. Protoc., **4**, 44-57.

Kanehisa, M., Sato, Y. and Kawashima, M. (2022): KEGG mapping tools for uncovering hidden features in biological data. Protein Sci., **31**, 47-53.

Krämer, A., Green, J., Pollard, J. Jr. and Tugendreich, S. (2014): Causal analysis approaches in Ingenuity Pathway Analysis. Bioinformatics, **30**, 523-530.

Lipe, D.N., Elsayem, A., Cruz-Carreras, M.T., Thomas, J., Feliciano, A., Ren, J., Gaeta, S.M., Rajha, E., Manasanch, E., Kheder, E., Brock, P. and Reyes-Gibby, C. (2020): Characteristics of cancer patients with COVID-19 in a cancer hospital. Ann. Palliat. Med., **10**, 1763-1771.

More, S.A., Patil, A.S., Sakle, N.S. and Mokale, S.N. (2021): Network analysis and molecular mapping for SARS-CoV-2 to reveal drug targets and repurposing of clinically developed drugs. Virology, **555**, 10-18.

Pizzorno, A., Padey, B., Julien, T., Trouillet-Assant, S., Traversier, A., Errazuriz-Cerda, E., Fouret, J., Dubois, J., Gaymard, A., Lescure, F.-X., Dulière, V., Brun, P., Constant, S., Poissy, J., Lina, B., Yazdanpanah, Y., Terrier, O. and Rosa-Calatrava, M. (2020): Characterization and Treatment of SARS-CoV-2 in Nasal and Bronchial Human Airway Epithelia. Cell Reports Medicine, **1**, 100059.

Qi, Y.J., Jiao, Y.L., Chen, P., Kong, J.Y., Gu, B.L., Liu, K., Feng, D.D., Zhu, Y.F., Ruan, H.J., Lan, Z.J., Liu, Q.W., Mi, Y.J., Guo, X.Q., Wang, M., Liang, G.F., Lamont, R.J., Wang, H., Zhou, F.Y., Feng, X.S. and Gao, S.G. (2020): Porphyromonas gingivalis promotes progression of esophageal squamous cell cancer via TGFβ-dependent Smad/YAP/TAZ signaling. PLoS Biol., **18**, e3000825.

Schäfer, M., Dütsch, S., auf dem Keller, U., Navid, F., Schwarz, A., Johnson, D.A., Johnson, J.A. and Werner, S. (2010): Nrf2 establishes a glutathione-mediated gradient of UVB cytoprotection in the epidermis. Genes Dev., **24**, 1045-1058.

Schiller, J.T. and Lowy, D.R. (2021): An Introduction to Virus Infections and Human Cancer. Recent Results Cancer Res., **217**, 1-11.

Tanabe, S. (2020): The Therapeutic Mechanism of COVID-19. J. Clin. Med. Res., **2**(5), 1-3.

Tanabe, S., Quader, S., Ono, R., Cabral, H., Aoyagi, K., Hirose, A., Yokozaki, H. and Sasaki, H. (2020): Molecular Network Profiling in Intestinal- and Diffuse-Type Gastric Cancer. Cancers (Basel), **12**, 3833.

Tanabe, S., Quader, S., Ono, R., Cabral, H., Aoyagi, K., Hirose, A., Yokozaki, H. and Sasaki, H. (2021): Cell Cycle Regulation and DNA Damage Response Networks in Diffuse- and Intestinal-Type Gastric Cancer. Cancers (Basel), **13**, 5786.

The Cancer Genome Atlas Research Network (2014): Comprehensive molecular characterization of gastric adenocarcinoma. Nature, **513**, 202-209.

Zheng, W., Umitsu, M., Jagan, I., Tran, C.W., Ishiyama, N., BeGora, M., Araki, K., Ohashi, P.S., Ikura, M. and Muthuswamy, S.K. (2016): An interaction between Scribble and the NADPH oxidase complex controls M1 macrophage polarization and function. Nat. Cell Biol., **18**, 1244-1252.